Article

Prediction of Crack Width in RC Piles Exposed to Local Corrosion in Chloride Environment

Wei Shao , Xiaoqing He [*] , Danda Shi

Article

Prediction of Crack Width in RC Piles Exposed to Local Corrosion in Chloride Environment

Wei Shao [1], Xiaoqing He [2,*] and Danda Shi [1]

[1] College of Ocean Science and Engineering, Shanghai Maritime University, Shanghai 201306, P.R. China; weishao@shmtu.edu.cn; ddshi@shmtu.edu.cn
[2] Department of Hydraulic Engineering, School of Civil Engineering, Tongji University, Shanghai 200092, P.R. China; hexiaoqing0719@163.com
* Correspondence: hexiaoqing0719@163.com

Abstract: A novel prediction model for crack development of reinforced concrete (RC) piles with localized chloride corrosion in marine environment is proposed. A discrete method is used to solve the corrosion pit radius model and a crack extension model is developed to investigate the initiation and extension of cracks. The maximum corrosion degree of reinforced concrete pile is predicted according to the limit crack criterion, and finally a sensitivity analysis is carried out on the important parameters of crack extension. The results show that the radius of corrosion pit, the depth corrosion pit and cross-sectional area loss of reinforcement gradually increase as the corrosion level increases. The loss of local reinforcement section at crack initiation decreases with the increase of the ratio of concrete cover to initial diameter, and increases with the increase of pitting factor. The required pit depth for reinforcement cracking increases with the increase of the ratio of concrete cover thickness to diameter. The loss of cross-sectional area of reinforcement and the radius of corrosion pit increase with the increase of initial diameter of reinforcement. Increasing the pitting factor will reduce the pit depth and make the crack width develop faster before reaching the limit crack width. Increasing the concrete cover thickness can provide an improvement in the propagation of cracks. A comparative analysis shows that the localized corrosion pattern is more in conformity with marine engineering practice.

Keywords: localized corrosion; corrosion pit radius; steel section loss; crack extension; maximum corrosion level

1. Introduction

In recent years, the corrosion of reinforced concrete (RC) structures in marine environment has received great concern. RC structures can be affected by chloride, air, seawater splash, wind and other external factors during service, which can cause corrosion of reinforced concrete structures. Corrosion can produce some corrosion products on the surface of RC structures, which can cause the volume increase and create tensile stress around the reinforced concrete. When the maximum tensile strength exceeds the tensile stress of the concrete, the cracking of concrete cover initiates. The concrete cracking may cause early intrusion of local chloride ions and corrosion of reinforcement, Concrete cracking may cause early localized chloride ion ingress and reinforcement corrosion, corrosion-induced cracks penetrate the concrete cover and provide a way for corrosive media such as chloride ions and oxygen to rapidly enter the reinforcement [1,2]. The cracks start to spread outwards from the steel-concrete interface and finally lead to complete cracking of the concrete cover.

The mechanism of damage and crack expansion in RC structures caused by corrosion and expansion of reinforcement has always been a hot topic of research in this field. Reinforcement corrosion can affect the safety and durability of RC structures. Many scholars have studied the bearing capacity of RC structures locally corroded by chloride [3–9]. In the actual marine environment, chlorides generally penetrate into the concrete in one direction, and corrosion may start

from the outermost layer of the reinforcement, so the steel bar may not corrode uniformly in cross sections [10], Corrosion pits of varying sizes are randomly produced on the reinforcement surface. The development of corrosion pits is related to the generation of cracks. In fact, longitudinal cracks provide the clearest visual representation of steel corrosion. Shao et al. [11] proposed an analysis model for durability life of RC piles with chloride local corrosion considering the impact of crack growth stage on the structure. Guzmán and Gálvez [12] used embedded cohesive cracking finite element analysis to study the effect of localized corrosion on the cracking of concrete cover, deriving different cracking patterns. Kim and Kim [13] estimated the maximum corrosion depth of local corrosion of reinforcement considering chloride ion diffusion. Li et al. [14] conducted tests on pit corrosion of reinforcement in chloride ion corroded concrete and analyzed the relationship between pit depth, residual sectional area and area of the smaller planar principal moment of inertia and corrosion grade. Darowicki et al. [15] investigated localized corrosion of stainless steel using optical surface measurement technology and deduced the cumulative distribution function of pitting corrosion. Kioumarsi et al. [16] studied the influence of corrosion pit disturbance on the damage probability of reinforced concrete beams after localized corrosion. Vidal et al. [17] predicted the crack width of corrosion in reinforced concrete structures and proposed a relationship between reinforcement section loss and cracking. Zhang et al. [18] measured the crack initiation, maximum load, fracture energy and other parameters of short cut basalt fiber concrete through tests, and studied the crack resistance of concrete. Zhang et al. [19] presented a new model to predict steel corrosion from corrosion cracks based on the average steel section loss parameter. Li et al. [20] inferred a theoretical model for the corrosion crack width of reinforced concrete structures. Zhao et al. [21] presented a concrete cracking model to investigate stress and cracks in concrete cover caused by reinforcing steel corrosion. Many scholars have conducted a great number of studies on the corrosion initiation and concrete cracking of RC structures. Chernin and Val [22] provided a review of existing models for predicting corrosion-induced cracking times in concrete cover. Xu et al. [23] studied the cracking of concrete protective layers caused by non-uniform corrosion of reinforcement. In fact, defining the initiation of corrosion or the appearance of the first crack as the end of the functional life of a RC structure underestimates the real life of a reinforced concrete structure. This method of predicting the durability life of RC structures is too conservative. When cracks develop to the limit crack, the structure fails. Although the above studies have studied the development of corrosion cracks in reinforced concrete, these studies have not combined the pit depth, corrosion degree and crack development. To predict the durability life of RC structures partially corroded by chloride more comprehensively, the mechanism of corrosion crater development and crack propagation should be studied in depth. Therefore, it is very meaningful to study the development of cracks for the durability life prediction and repair of RC structures.

In this paper, a novel prediction model for crack development of RC piles with localized chloride corrosion in marine environment is proposed. The maximum corrosion degree of RC pile is predicted according to the limit crack criterion. A discrete method is used to solve the corrosion pit radius model, then crack initiation and extension are investigated based on the crack extension model, and finally a sensitivity analyses were conducted on the important parameters of crack extension.

2. Localized corrosion modelling

2.1. Geometry model

RC piles exposed to the marine environment are easily corroded by chloride ions. The corrosion of RC structure is generally divided into uniform corrosion and local corrosion, and local corrosion is the key factor for predicting the durability life of RC piles. When reinforced concrete is corroded, corrosion pits are created on the surface of the reinforcement. The location and shape of these corrosion pits are formed randomly and they are related to factors such as the environment and the level of corrosion. In this paper, the non-uniform corrosion model proposed by Alami et al. [24] is used to study the development of corrosion crater. It is assumed that the shape of the corrosion pit is semi-circular, and the center of the corrosion crater is located at the edge of the reinforcement.

2.2. Modelling of corrosion pits

As corrosion process proceeds, corrosion products can be produced on the surface of reinforcement, and corrosion products can expand on the surface of reinforcement. In this paper, the distribution of corrosion pits on the surface of reinforcement is regarded as a simple geometric distribution. As shown in Figure 1, it is assumed that the centre O' of the corrosion crater is directly above the center O of the reinforcement. The intersection points of corrosion pit and reinforcement are Q and Q', respectively, the intersection of OO' and QQ' is I, and the radius of corrosion pit is R'. According to Figure 1, the shadow area is the corrosion pit area, which is composed of two semicircles with different radii. The pit area is the sum of the areas of zone 1 and zone 2.
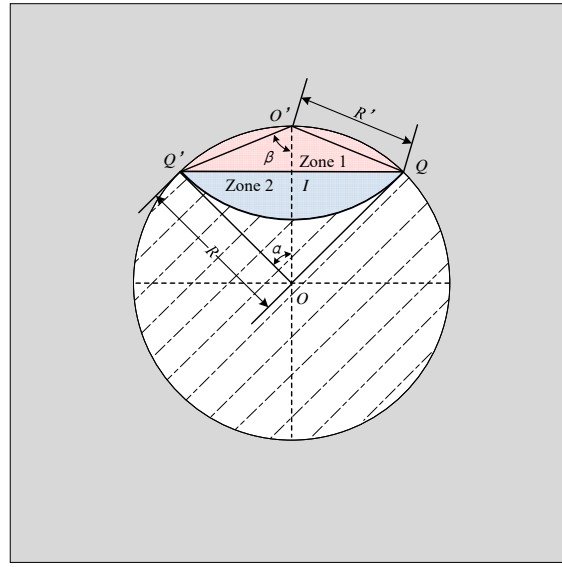

Figure 1. Area loss of reinforcement.

In the corrosion pit model, it is assumed that

$$IQ = IQ' \tag{1}$$

The area of zone 1 can be expressed as

$$A_1 = A_{S_{OQQ'}} - A_{T_{OQQ'}} \tag{2}$$

The area of triangle OQQ' obtained from geometric knowledge can be expressed as

$$A_{T_{OQQ'}} = IQ \times IO \tag{3}$$

IO can be expressed as

$$IO = \sqrt{OQ^2 - QI^2} = \sqrt{R^2 - R'^2} \tag{4}$$

Therefore, the area of the triangle OQQ' is expressed as

$$A_{T_{OQQ'}} = R' \times \sqrt{R^2 - R'^2} \tag{5}$$

The expression for the area of the sector OQQ' can be expressed as

$$A_{S_{OQQ'}} = \frac{2\pi R^2 \alpha}{360} \tag{6}$$

The angle α can be expressed as

$$\sin\alpha = \frac{R'}{R} \tag{7}$$

Therefore, the expression for α is

$$\alpha = \arcsin\frac{R'}{R} \tag{8}$$

Therefore, the area of sector OQQ' is calculated as

$$A_{S_{OQQ'}} = \frac{2\pi R^2}{360}\cdot\arcsin\frac{R'}{R} \tag{9}$$

In summary, the area of region 1 is obtained as

$$A_1 = A_{S_{OQQ'}} - A_{T_{OQQ'}} = \left(\frac{2\pi R^2}{360}\cdot\arcsin\frac{R'}{R}\right) - \left(R'\times\sqrt{R^2 - R'^2}\right) \tag{10}$$

Based on the same analysis method, the area of zone 2 can be obtained as

$$A_2 = A_{S_{O'QQ'}} - A_{T_{O'QQ'}} \tag{11}$$

IO' can be expressed as

$$IO' = OO' - OI = R - \sqrt{R^2 - R'^2} \tag{12}$$

The relationship between angle β and angle α is given by

$$\beta = 90° - \alpha \tag{13}$$

Therefore, the area of the sector $O'QQ'$ is obtained as

$$A_{S_{O'QQ'}} = \frac{2\pi R'^2}{360}\left(90° - \alpha\right) \tag{14}$$

The area of triangle $O'QQ'$ is given by

$$A_{T_{O'QQ'}} = R'\times\left(R - \sqrt{R^2 - R'^2}\right) \tag{15}$$

According to Eq. (14) and Eq. (15), the area of zone 2 is

$$A_2 = A_{S_{O'QQ'}} - A_{T_{O'QQ'}} = \frac{2\pi R'^2}{360}\cdot\left(90 - \alpha\right) - R'\times\left(R - \sqrt{R^2 - R'^2}\right) \tag{16}$$

Therefore, the corrosion pit area can be expressed as

$$\Delta A_s = A_1 + A_2 = 2\pi\left[\frac{R'^2}{360}\cdot(90 - \alpha) + \frac{R^2}{360}\cdot\alpha\right] - R'\cdot\left[\sqrt{R^2 - R'^2} + \left(R - \sqrt{R^2 - R'^2}\right)\right] \tag{17}$$

Eq. (17) can be simplified as

$$\Delta A_s = 2\pi\left[\frac{R'^2}{360}\cdot\left(90° - \alpha\right) + \frac{R^2}{360}\cdot\alpha\right] - RR' \tag{18}$$

where ΔA_s is the area of the corrosion pit and denotes the loss of cross-sectional area of the reinforcement, R' is the corrosion pit radius and R is the initial radius of the reinforcement. In general, the degree of corrosion of reinforced concrete piles is expressed as the percentage mass loss of reinforcement ρ, and ρ can be calculated as

$$\rho = \frac{M_1 - M_2}{M_1} \tag{19}$$

where M_1 and M_2 are the masses of the reinforcement bars before corrosion and the mass after corrosion, respectively. Eq. (19) can be rewritten as [25]

$$\rho = \frac{M_1 - M_2}{M_1} = \frac{\rho_{rebar} \cdot \Delta A_s}{\rho_{rebar} \cdot A_{rebar}} = \frac{\Delta A_s}{A_{rebar}} \tag{20}$$

According to Eq. (18) and Eq. (20), the following equation can be obtained as

$$\rho A_{rebar} = 2\pi \left[\frac{R'^2}{360}\left(90° - \alpha\right) + \frac{R^2}{360}\alpha \right] - RR' \tag{21}$$

where ρ is the degree of corrosion of the reinforcement, and A_{rebar} is the initial area of the reinforcement. Eq. (21) involves two unknown parameters ρ and R', when the degree of corrosion ρ is known, the radius of pit radius R' can be obtained for different corrosion degrees. However, since the unknown parameter R' is present in the trigonometric function, the radius of the corrosion pit cannot be solved by simple reduction. The relevant programming software is used to scatter countless points in the feasibility domain of radius R' to find the closest solution. The variation of the corrosion pit radius R' and the loss of reinforcement cross-sectional area ΔA_s with the degree of corrosion are analyzed. Because the discrete approach generates a certain amount of error, the model calculation error E is also analyzed in this study.

2.3. Analysis of crack width

After the onset of cracking in RC structures, the corrosion products on the surface can first fill the local pores and then be deposited at the interface between the reinforcement and the concrete. The depth of corrosion pit required for reinforcement cracking is calculated by [26]

$$x_0 = 7.53 + 9.32\frac{c}{D_0} \tag{22}$$

where x_0 is the corrosion pit depth required for cracking, c is the concrete cover thickness (mm) and D_0 is the initial diameter of the reinforcement. The above equation shows that the depth of corrosion pit required for cracking is related to the ratio of the concrete cover thickness and the initial diameter of the reinforcement. The relationship between the depth of corrosion crater and reinforcement cross-section loss can be obtained by [17]

$$x = \frac{D_0}{\alpha}\left[1 - \sqrt{1 - \frac{\Delta A_s}{A_{rebar}}} \right] \cdot 10^3 \tag{23}$$

where α is the pitting factor, is the ratio of localized corrosion depth to uniform corrosion depth, $\alpha=2$, for uniform corrosion, $4<\alpha<8$, for localized corrosion, D_0 is the initial diameter of the reinforcement (mm), A_{rebar} is the initial area of the reinforcement and ΔA_s is the loss of reinforcement cross-section. The relationship between the corrosion pit depth x and the corrosion pit radius R' is shown in Fig. 4. According to Eqs. (22) and (23), the local steel section loss at the beginning of cracking can be obtained as [19]

$$\Delta A_{s0} = A_{rebar}\left[1 - \left[1 - \frac{\alpha}{D_0}\left(7.53 + 9.32\frac{c}{D_0} \right) \cdot 10^{-3} \right]^2 \right] \tag{24}$$

It should be noted that the local reinforcement section loss at the onset of cracking obtained by Eq. (24) is obtained without taking into account the properties of the concrete. Based on the

experimental data, a linear regression formula obtained by Vidal et al. [17] is used for predicting crack width as

$$w = K\left(\Delta A_s - \Delta A_{s0}\right) \tag{25}$$

where ΔA_{s0} is the loss of local steel cross-section at the beginning of cracking, and K is the slope of the curve (K =0.0575). According to the limit crack criterion, when the crack width exceeds the limit crack value, the reinforced concrete pile loses stability.

3. Analysis results

In this paper, the selected limit crack width is w_{lim}=0.4 mm. The values of model parameters used in this analysis are shown in Table 1. According to Eq. (22), the pit depth at the beginning of reinforcement cracking is 0.054 mm, according to Eq. (24), the local steel section loss at the beginning of cracking is 4.73 mm². The relationship between the radius of the corrosion pit and the loss of reinforcement cross-section with the degree of corrosion is shown in Figure 2. When the corrosion degree increases, the corrosion pit radius gradually increases and the reinforcement section loss gradually increases. This is consistent with the findings of the experiment by Li et al. [14]. The error analysis caused by solving the corrosion pit radius with discrete method is shown in Figure 3. The error varies randomly and irregularly as the corrosion level increases from 1% to 16%, while each error is very small, therefore, the influence of the error formed by the discrete method on the results can be ignored. Figure 4 shows the relationship between corrosion crater radius and corrosion crater depth. The depth of corrosion pit increases with increasing pit radius.

Table 1. Values of main parameters used in the analysis.

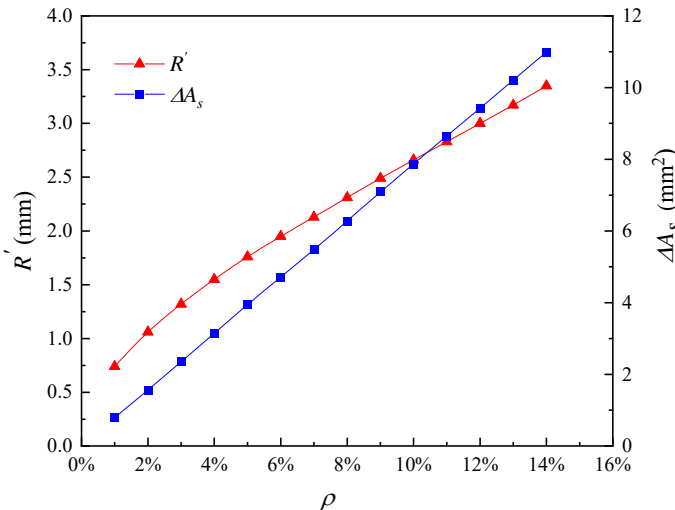| Parameters	Unit	Values	Description	Reference
a	mm	190	Inner radius of pile	
b	mm	300	Outside radius of pile	
D_0	mm	10	Initial diameter of steel bar	
c	mm	50	Concrete cover thickness	
w_{lim}	mm	0.4	Limit crack width	[27]
α		5.65	Pitting factor	[17]
K		0.0575	slope of curve	[28]

Figure 2. Influence of corrosion degree on radius of corrosion pit and cross-sectional area loss of reinforcement.
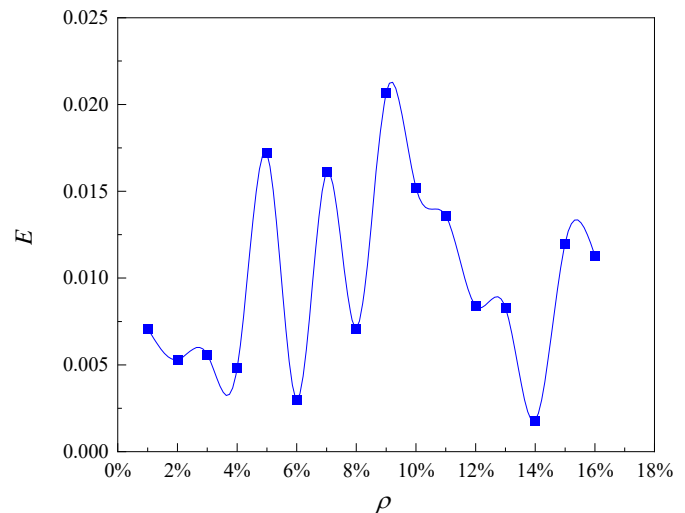
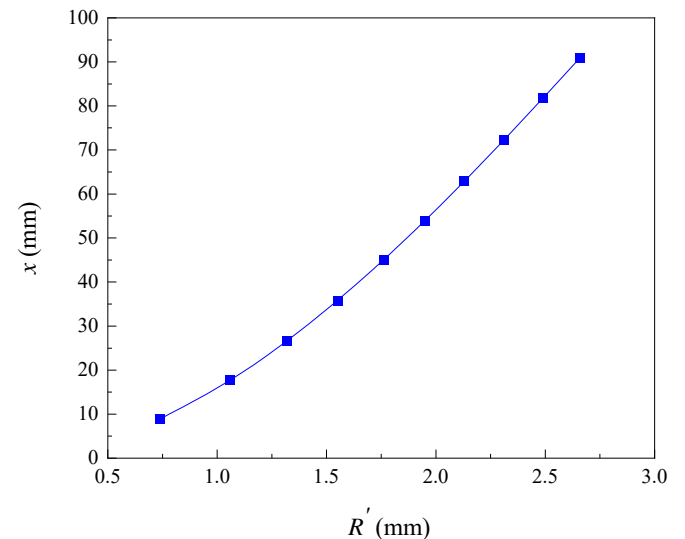**Figure 3.** Calculation error of corrosion pit radius.

Figure 4. Influence of pit radius variation on corrosion pit depth.

The effect of pitting factor on corrosion crater depth is shown in Figure 5. When the corrosion degree is 8%, the pit depth decreases from 115.50 mm to 57.75 mm as the pitting factor increases from 4 to 8. The crater depth decreases with the increase of pitting factor. This is because when the corrosion degree is certain, the cross-sectional loss of reinforcement is also a fixed value, and the depth of the corrosion pit is inversely proportional to the pitting factor. When the pitting factor is 6, the pit depth increases from 50.81 mm to 76.99 mm as the corrosion degree increases from 6% to 9%. The corrosion degree increases from 6% to 7%, from 7% to 8%, and from 8% to 9%, the pit depth increases by 16.53%, 14.69%, and 13.27%, respectively. The depth of corrosion crater increases slowly. This is because with the increase of corrosion level, the local corrosion of reinforcement becomes more and more serious. The corrosion products generated by corrosion attach to the surface of reinforcement, and blocks the flow of media required for corrosion such as chlorine ion and oxygen, thus slowing down the development of corrosion to a certain extent.

The effect of the pitting factor on the crack width is shown in Figure 6. When the corrosion degree is 9%, the crack width reduces from 0.21 mm to 0.025 mm as the pitting factor increases from 4 to 8. The crack width decreases with the increase of pitting factor. When the pitting factor is 5, the crack width increases from 0.03 mm to 0.17 mm as the corrosion degree increases from 6% to 9%. The crack width increases 4.67 times. The crack width increases with the increase of corrosion degree. This is because with the progress of corrosion, air, oxygen and other corrosive media are sufficient,

and corrosion will develop rapidly at the beginning. The crack width will expand rapidly before reaching the limit crack width, but after the crack width reaches the threshold, the corrosion rate will slow down because the accumulation of corrosion products restricts the flow of air and so on.
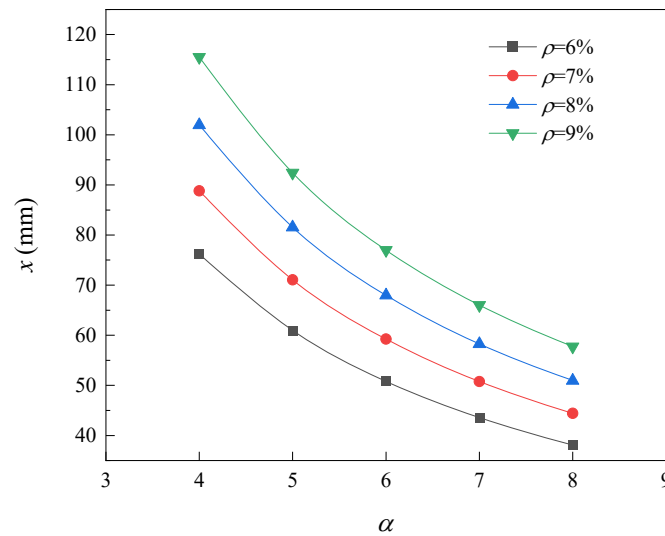

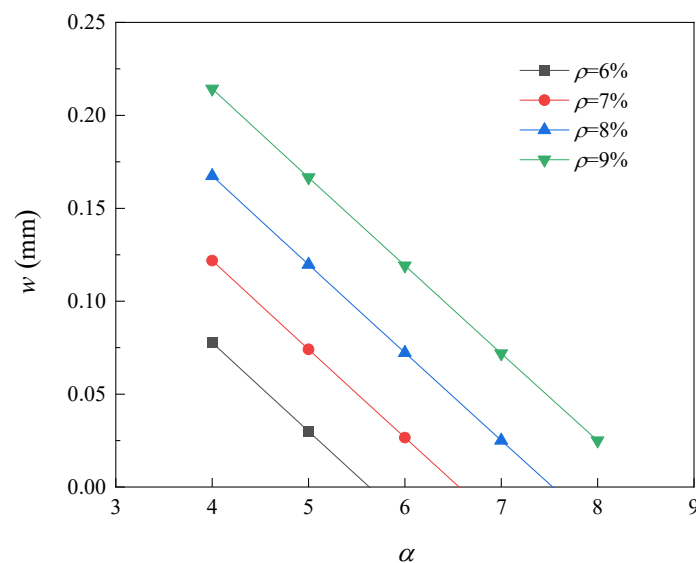**Figure 5.** Influence of pitting factor on pit depth.

Figure 6. Effect of pitting factor on crack width.

The influence of the concrete cover thickness on the required pit depth at the initiation of reinforcement cracking is shown in Figure 7. When concrete cover thickness increases from 40 mm to 60 mm, the corrosion pit depth at the beginning of reinforcement cracking increases from 44.81 mm to 63.45 mm. The depth of the pit required for the initiation of reinforcement cracking increases with the concrete cover thickness. This is because increasing the concrete cover thickness not only increases the diffusion path of the chloride, but also decreases the tensile stresses on the outer surface of the concrete cover due to the radial expansion of the corroded reinforcement, thus delaying the initiation of cracking the concrete cover.
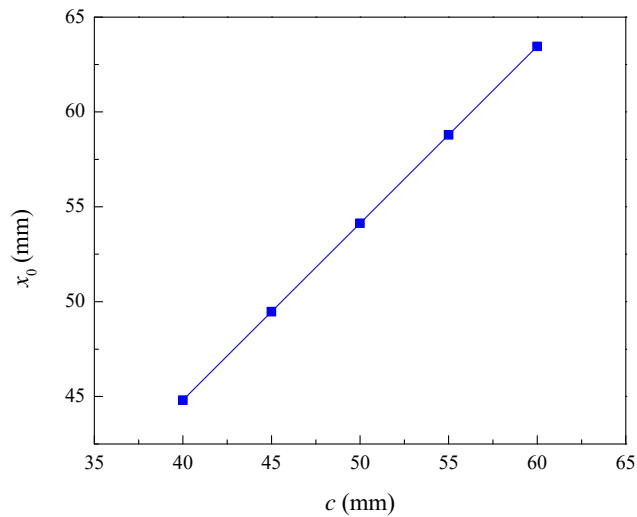
Figure 7. Influence of concrete cover thickness on pit depth during cracking.

The influence of the thickness of concrete cover on crack width is shown in Figure 8. When corrosion degree is 8%, the crack width decreases from 0.14 mm to 0.04 mm as the concrete cover thickness increases from 40 mm to 60 mm. The crack width decreases with the increase of concrete cover thickness. This is because the increase in the thickness of the concrete cover improves the impermeability, corrosion resistance and other durability of the reinforced concrete, so the crack expansion is improved. Generally speaking, the greater the thickness of the concrete cover, the longer it takes for the external corrosive medium to reach the surface of the steel, the less likely it is for the reinforcement to rust, and the better the durability of the concrete. However, the concrete cover should not be too thick, as the shrinkage and temperature stresses are not well controlled during the hardening process.
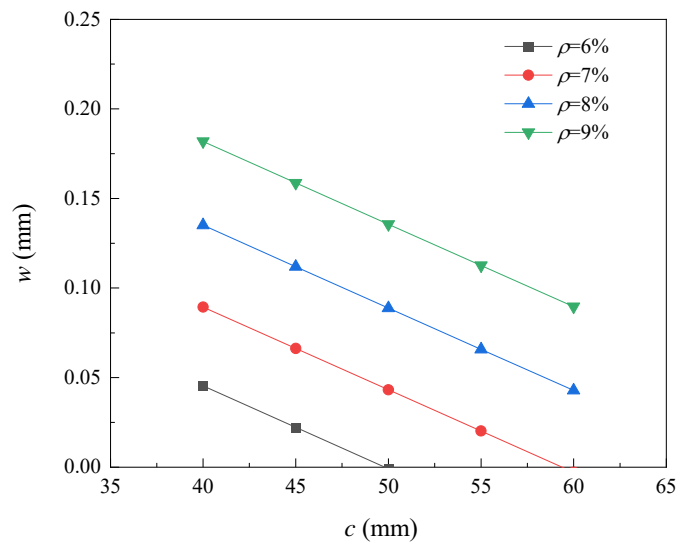

Figure 8. Effect of concrete cover thickness on crack width.

The effect of initial diameter of reinforcement on the radius of corrosion pit and the loss of reinforcement section is shown in Figure 9. When the corrosion degree is 6%, the radius of corrosion pit increases from 1.56 mm to 3.12 mm with the reinforcement diameter increasing from 8 mm to 16 mm. At the same corrosion degree, the radius of corrosion pit tends to increase with the increase of initial diameter of reinforcement. When the initial diameter is 10 mm, the corrosion pit radius increases from 1.95 mm to 2.49 mm as corrosion level increases from 6% to 9%. At the same initial

diameter, the radius of corrosion pit tends to increase with the increase of corrosion degree. This shows that the corrosion radius and the loss of cross-sectional area of reinforcement increase with the increase of initial diameter of reinforcement.
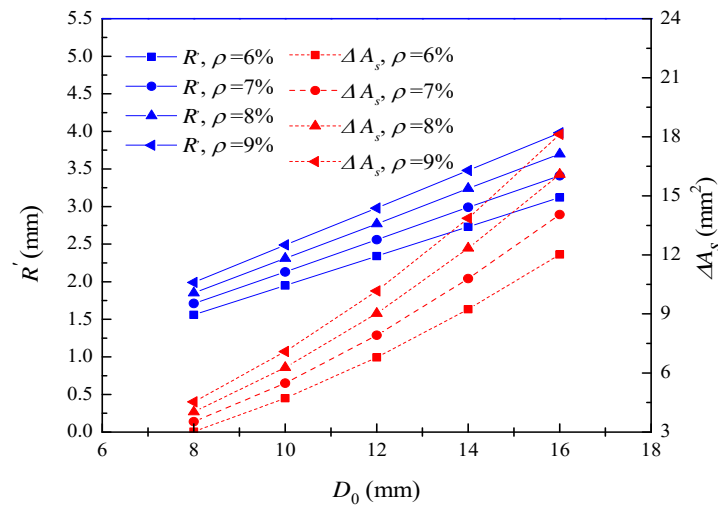

Figure 9. Effect of initial diameter on corrosion pit radius and loss of reinforcement cross-section.

Figure 10 shows the influence of initial diameter of reinforcement on the depth of corrosion pit at the beginning of reinforcement cracking and in the process of corrosion. When the corrosion degree is 6%, 7%, 8% and 9%, the corrosion pit depth increases from 43.16 mm to 86.32 mm, from 50.61 mm to 100.71 mm, from 57.85 mm to 115.70 mm, and from 65.31 mm to 130.61 mm, as the initial diameter of reinforcement increases from 8 mm to 16 mm. At the same corrosion degree, the pit depth increases with the increase of the initial diameter of the reinforcement. When the initial diameter of the reinforcement increases from 8 mm to 16 mm, the required corrosion pit depth for cracking of the reinforcement decreases from 65.78 mm to 36.66 mm. The depth of corrosion pit required for reinforcement cracking reduces as the initial diameter of the reinforcement increases.
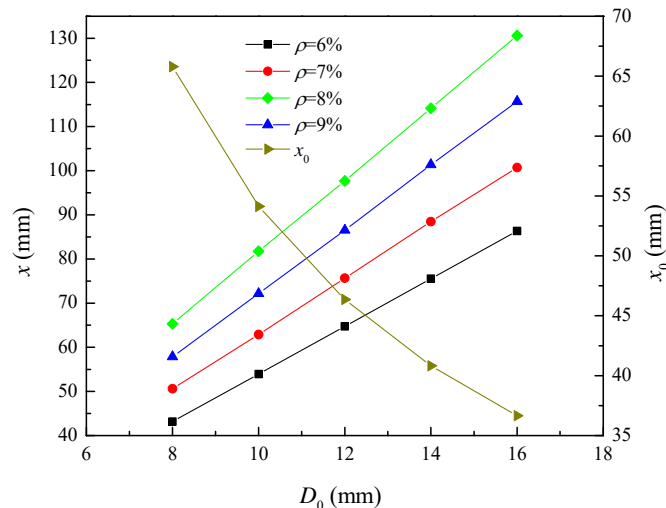

Figure 10. Influence of initial diameter on the pit depth at the initiation of cracking and the pit depth during corrosion.

The relationship between the localized reinforcement cross-section loss at the beginning of reinforcement cracking and the ratio of concrete cover thickness to initial diameter is shown in Figure 11(a). The localized loss of reinforcement cross-section at the onset of cracking decreases as the ratio of concrete cover thickness to initial diameter increases. The relationship between local reinforcement section loss and pitting factor at the beginning of reinforcement cracking is shown in Figure 11(b). The localized reinforcement cross-section loss at the beginning of reinforcement cracking increases

with the pitting factor. This is because the increase of pitting factor means that the ratio of local corrosion degree to uniform corrosion degree increases, and the local corrosion degree increases, and then the loss of cross sectional area of reinforcement at the beginning of reinforcement cracking increases.
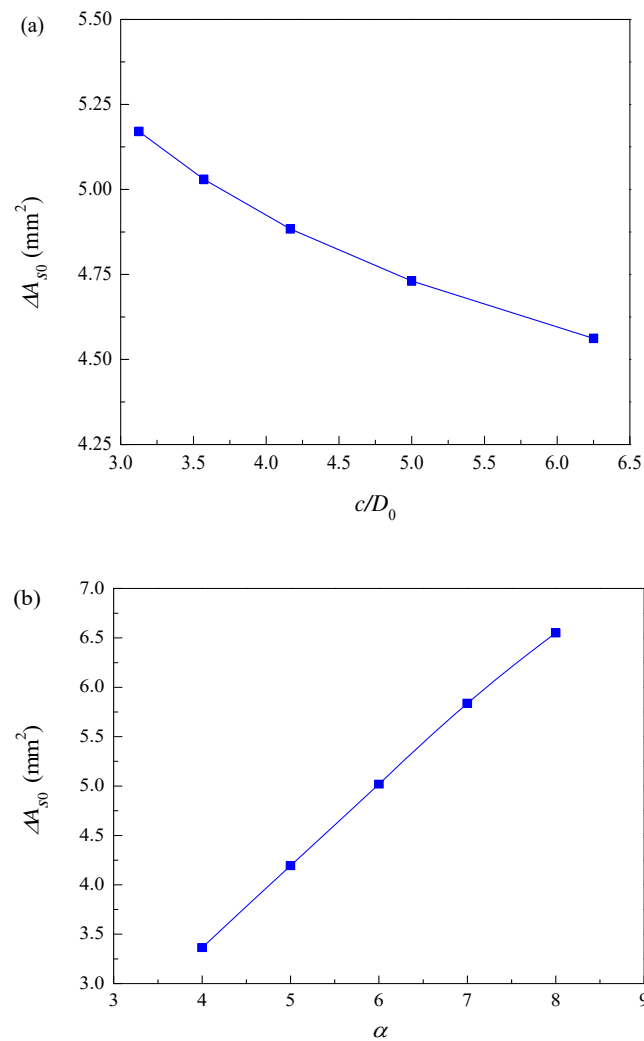
Figure 11. Influence of factors on the local reinforcement cross-section loss at the initiation of cracking: (a) the ratio of cover thickness to initial diameter; and (b) pitting factor.

The influence of corrosion degree on crack width is shown in Figure 12(a). When the corrosion level is approximately 15%, the crack width reaches the ultimate crack width of 0.4 mm, and the structure becomes unstable. The influence of the loss of cross-sectional area of reinforcement on the crack width is shown in Figure 12(b). When the crack width reaches the limit crack width, the loss of cross-sectional area of reinforcement is about 11.79 mm^2. The crack width increases with the increase of corrosion degree. This is because the reinforcement corrosion becomes more serious with the increase of corrosion degree. The crack gradually expands with the reinforcement corrosion until the structure is unstable.
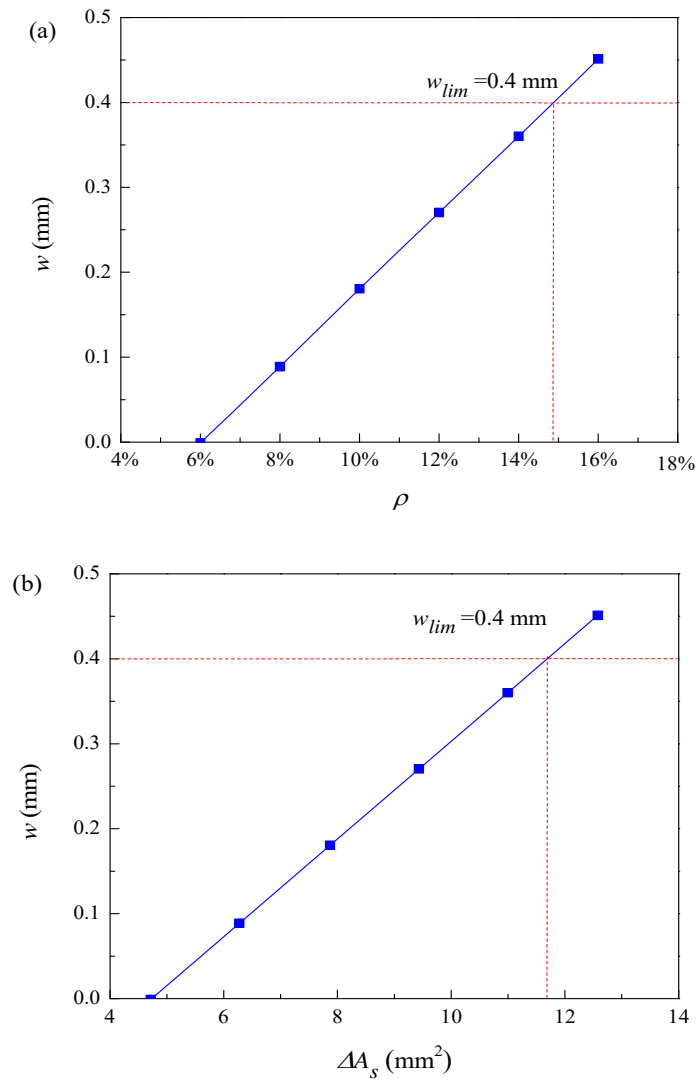
Figure 12. Effect of different factors on crack width: (a) corrosion degree; and (b) Loss of reinforcement cross-sectional area.

Figure 13 shows the influence of initial diameter of reinforcement on model error of corrosion pit radius. As the corrosion level increases from 1% to 16%, the error curves follow very similar trends for initial steel diameters of 8 mm, 10 mm and 12 mm. The error varies within the range from 0 to 2%. Therefore, it can be concluded that the initial diameter of reinforcement has little effect on the variation trend of the error of the pit radius model, and the error caused by the solution of the pit radius model can be ignored.
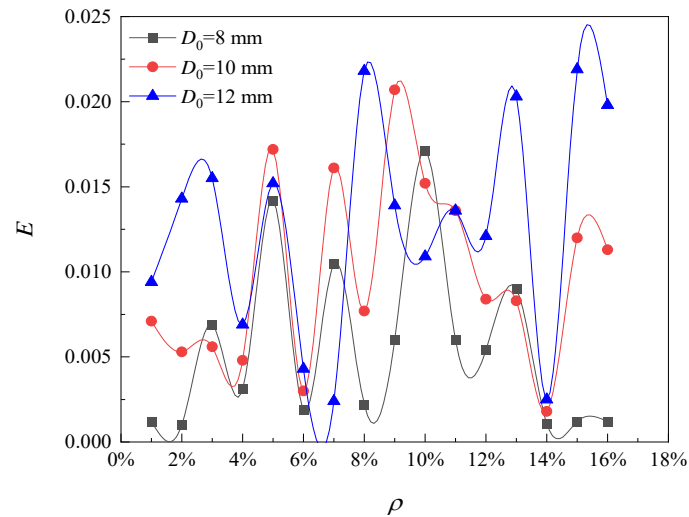
Figure 13. Effect of diameter change on error.

4. Discussion

Comparison of localized and uniform corrosion: Kim and Kim [13] carried out a numerical analysis of localized corrosion (two-dimensional corrosion) of reinforced concrete structures. The results show that the depth of localized corrosion is 3.5 times greater than the depth of uniform corrosion after 3.5 years from the onset of corrosion. The results of Santiago and Jaime's study show that the concrete surface cracking time in localized corrosion mode is earlier and the vertical surface displacement is much greater than in uniform corrosion [12]. It has been shown that in the localized corrosion mode, cracks appear earlier on the concrete surface and the pressure to crack the concrete surface is much less than in the uniform corrosion mode. In addition, localized corrosion requires less loss of reinforcement section and shorter periods to study the limit state of the concrete structure [8,10,29]. In conclusion, the uniform corrosion model to study the corrosion of reinforced concrete structures is too conservative, and there is a gap with the actual engineering conditions. The cracking time of the concrete surface, the crack initiation time and the time when the cracks reach the ultimate crack are much later in the uniform corrosion model than in the localized corrosion model. Therefore, in order to be more relevant to the actual marine engineering, the crack analysis of reinforced concrete structures in localized corrosion mode should be developed as much as possible. This paper only proposes a new method for predicting cracks in concrete piles under localized corrosion of chloride in marine environment, and the predicted results in this paper are in conformity with many experimental results. However, the shape, size and spatial distribution of the specific corrosion pits and cracks need to be investigated in more depth.

5. Conclusions

In this paper, a novel prediction model for crack development of RC piles with local chloride corrosion in marine environment is proposed. The generation and extension of cracks are studied and a sensitivity analysis of the important parameters of the cracking phase is carried out. Therefore, the following conclusions can be obtained.

(1) The radius of corrosion pit, loss of cross-sectional area of reinforcement and corrosion pit depth increase as the corrosion level increases. The corrosion pit depth decreases with increasing pitting factor and the crack width develops more rapidly before the ultimate crack width is reached. The increased thickness of the protective concrete cover delays the cracking of the concrete surface and provides an improvement in the propagation of cracks.

(2) The required pit depth for reinforcement cracking increases with the increase of the ratio of concrete cover thickness to diameter. The loss of cross-sectional area of reinforcement and the radius of corrosion pit increase with the increase of initial diameter of reinforcement. The loss of local

reinforcement section at the beginning of reinforcement cracking decreases with the increase of the ratio of concrete cover thickness to initial diameter, and increases with the increase of pitting factor.

(3) According to the limit crack criterion, the maximum corrosion degree of reinforced concrete pile is about 15%. The error caused by the discrete method can be ignored.

(4) A comparative analysis of the results of existing studies shows that chloride corrosion of reinforced concrete piles under the assumption of uniform corrosion is too conservative and that localized corrosion would be more in conformity with engineering practice. This paper only proposes a new method to predict the cracking of concrete piles by localized corrosion of chloride in the marine environment, and the predicted results are consistent with many experimental results. However, the shape, size and spatial distribution of specific corrosion pits and cracks need to be developed for more in-depth study.

References

1. Zhao, Y.X.; Wu, Y.Y.; Jin, W.L. Distribution of millscale on corroded steel bars and penetration of steel corrosion products in concrete. *Corrosion Science*. 2013, 66, 160–168.
2. Chao, Z.M.; Dang, Y.B.; Pan, Y.; Wang, F.Y.; Wang, M.; Zhang, J.; Yang, C.X. Prediction of the shale gas permeability: A data mining approach. *Geomechanics for Energy and the Environment*, 2023, 33, 100435.
3. Cao, C. 3D simulation of localized steel corrosion in chloride contaminated reinforced concrete. *Construction and Building Materials*. 2014, 72, 434–443.
4. Chen, E.; Berrocal, C.G.; Fernandez, I.; Löfgren, I.; Lundgren, K. Assessment of the mechanical behaviour of reinforcement bars with localized pitting corrosion by digital image correlation. *Engineering Structures.* 2020, 219, 110936.
5. Moreno, E.; Cobo, A.; Palomo, G.; González, N. Mathematical models to predict the mechanical behavior of reinforcements depending on their degree of corrosion and the diameter of the rebars. *Construction and Building Materials.* 2014, 61, 156–163.
6. Tang, F.J.; Lin; Z.B.; Chen, G.D.; Yi, W.J. Three-dimensional corrosion pit measurement and statistical mechanical degradation analysis of deformed steel bars subjected to accelerated corrosion. *Construction and Build Materials.* 2014, 70, 104–117.
7. Liu, J.; Wang, Z.G.; Zhang, R.B.; Du, X.L. Mesoscopic simulation on flexural behavior of single-way reinforced concrete slab with rebars subjected to localized corrosion. *Structures.* 2021,31, 815–827.
8. Xia, N.; ASCE, A.M.; Ren, Q.W.; ASCE, M.; Liang, R.Y.; ASCE, F.; Payer, J.; Patnaik, A.; ASCE, M. Nonuniform corrosion-induced stresses in steel-reinforced concrete. *Journal of Engineering Mechanics.* 2012, 138, 338–346.
9. Zhao, Y.X.; Hu, B.Y.; Yu, J.; Jin, W.L. Non-uniform distribution of rust layer around steel bar in concrete. *Corrosion Science*. 2011, 53, 4300–4308.
10. Jang, B.S.; Oh, B.H. Effects of non-uniform corrosion on the cracking and service life of reinforced concrete structures. *Cement and Concrete Research*. 2010, 40, 1441–1450.
11. Shao, W.; He, X.Q.; Shi, D.D. Durability life prediction of RC piles subjected to localized corrosion in chloride environments. *Engineering Failure Analysis*. 2022,136, 106184.
12. Guzmán, S.; Gálvez. J. C. Modelling of concrete cover cracking due to non-uniform corrosion of reinforcing steel. *Construction and Building Materials.* 2017, 155, 1063–1071.
13. Kim, C.-Y.; Kim, J.-K. Numerical analysis of localized steel corrosion in concrete. *Construction and Building Materials.* 2008, 22, 1129–1136.
14. Li, D.W.; Ren, W.; Li, L.; Guan, X.T.; Mi, X.M. Pitting corrosion of reinforcing steel bars in chloride contaminated concrete. *Construction and Building Materials.* 2019, 199, 359–368.

15. Darowicki, K.; Mirakowski, A.; Krakowiak, S. Investigation of pitting corrosion of stainless steel by means of acoustic emission and potentiodynamic methods. *Corrosion Science.* 2003, 45, 1747–1756.
16. Kioumarsi, M.M.; Hendriks, M.A.N.; Kohler, J. Geiker, M.R. The effect of interference of corrosion pits on the failure probability of a reinforced concrete beam. *Engineering Structures.* 2016, 114, 113–121.
17. Vidal, T.; Castel, A.; François, R. Analyzing crack width to predict corrosion in reinforced concrete. *Cement and Concrete Research.* 2004, 34, 165–174.
18. Zhang, W.B.; Shi, D. D.; Shen, Z. Z; Zhang, J.; Zhao, S.; Gan, L.; Li, Q. M.; Chen, Y. S.; Tang, P. Influence of chopped basalt fibers on the fracture performance of concrete subjected to calcium leaching. *Theoretical and Applied Fracture Mechanics.* 2023, 125, 103934.
19. Zhang, R.J.; Castel, A.; François, R. Concrete cover cracking with reinforcement corrosion of RC beam during chloride-induced corrosion process. *Cement and Concrete Research.* 2010, 40, 415–425.
20. Li, C.Q.; Lawanwisut, W.; Zheng, J.J.; Kijawatworawet, W. Crack width due to corroded bar in reinforced concrete structures. *International Journal of Materials & Structural Reliability.* 2005, 3, 87–94.
21. Zhao, Y. X.; Yu, J.; Jin, W.L. Damage analysis and cracking model of reinforced concrete structures with rebar corrosion. *Corrosion Science.* 2011, 53, 3388–3397.
22. Chernin, L.; Val, D. Prediction of corrosion-induced cover cracking in reinforced concrete structures. *Construction and Building Materials.* 2010, 25, 1584–1869.
23. Xu, G.; Wei, J.; Liu, H.Q. The experimental study of the non-uniform corrosion of steel bars. *Journal of Huazhong University of Science and Technology (Nature Science Edition).* 2006, 34, 111–114.
24. Eliass, E.A.; Fekak, F.E.; Garibaldi, L.; Ahmed, E. A numerical study of pitting corrosion in reinforced concrete structures. *Journal of Building Engineering.* 2021, 43, 102789.
25. Sun, J.; Ding, Z.H.; Huang, Q. Corrosion fatigue life prediction for steel bar in concrete based on fatigue crack propagation and equivalent initial flaw size. *Construction and Building Materials.* 2019, 195, 208–217.
26. Alonso, C.; Andrade, C.; Rodriguez, J.; Diez, J.M. Factors controlling cracking of concrete affected by reinforcement corrosion. *Materials and Structures.* 1998, 31, 435–441.
27. Stewart, M.G.; Mullard, J.A. Spatial time-dependent reliability analysis of corrosion damage and the timing of first repair for RC structures. *Engineering Structures.* 2007, 29, 1457–1464.
28. Stewart, M.G. Spatial variability of pitting corrosion and its influence on structural fragility and reliability of RC beams in flexure. *Structures Safety.* 2004, 26, 453–470.
29. Zhao, Y.X.; Karimi, A.R.; Wong, H.S.; Hu, B.Y.; Buenfeld, N.R.; Jin, W.L. Comparison of uniform and non-uniform corrosion induced damage in reinforced concrete based on a Gaussian description of the corrosion layer. *Corrosion Science.* 2011, 53, 2803–2814.